

Thermal Properties of Yttria-Stabilized Zirconia (YSZ)

J. Spišiak, M. Hartmanová

Institute of Physics, Slovak Academy of Sciences, 84228 Bratislava, Slovak Republic

G. G. Knab

Institute of Crystallography, Russian Academy of Science, 117333 Moscow, Russia

&

S. Krcho

ZSE Electrocarbon, 95522 Topolčany, Slovak Republic

(Received 15 June 1992; revised version received 30 October 1992; accepted 10 December 1992)

Abstract

The thermal properties and microhardness of yttria-stabilized zirconia (YSZ) and YSZ doped with 1 wt% WO_3 have been investigated at 300 K. The thermal conductivity λ of YSZ doped with WO_3 has a higher value than without the tungsten doping ($\lambda_{\text{YSZ}} = 1.26 \pm 0.05$; $\lambda_{\text{YSZ}+\text{WO}_3} = 1.65 \pm 0.15$ (W/m K)). A similar influence of tungsten addition was found in the case of the microhardness H . $H_{\text{YSZ}+\text{WO}_3}$ is 12–15% higher than H_{YSZ} . The thermal properties in the surface layers and in the bulk of the sample are different. A similar difference was observed in the case of the microhardness H . Doping sharply decreases H in the surface layer, practically down to the level of the bulk value. The results allow the assumption that the doping of YSZ samples with WO_3 essentially changes, in a similar way, the structure of surface layer in the ceramic grains as in the single crystals.

Die thermischen Eigenschaften und die Mikrohärte von Yttriumoxid stabilisiertem Zirkoniumoxid (YSZ) und YSZ dotiert mit 1 Gew.% WO_3 wurde bei einer Temperatur von 300 K untersucht. Die thermische Leitfähigkeit, λ , von WO_3 dotiertem YSZ ist höher als die Leitfähigkeit des undotierten YSZ ($\lambda_{\text{YSZ}} = 1.26 \pm 0.05$; $\lambda_{\text{YSZ}+\text{WO}_3} = 1.65 \pm 0.15$ (W/m K)). Ein ähnlicher Effekt der Wolframdotierung konnte auch für die Mikrohärte H beobachtet werden. $H_{\text{YSZ}+\text{WO}_3}$ ist 12–15% höher als H_{YSZ} . Die thermischen Eigenschaften der Oberflächenschicht und der massiven Probe sind verschieden. Ein ähnlicher Unterschied wurde für die Mikrohärte H beobachtet.

Durch die Dotierung wird H in der Oberflächenschicht deutlich verringert, praktisch bis zum Wert der massiven Probe. Aufgrund der Ergebnisse kann angenommen werden, daß das Dotieren von YSZ Proben mit WO_3 die Struktur der Oberflächenschicht der Keramikkörner und des Einkristalls im wesentlichen in gleicher Weise verändert.

Les propriétés thermiques et la microdureté de zircons stabilisés à l'oxyde d'yttrium (YSZ) et de YSZ dopées par 1% en poids de WO_3 ont été étudiées à 300 K. La conductivité thermique de YSZ dopée par WO_3 est plus grande que celle mesurée en l'absence de tungstène ($\lambda_{\text{YSZ}} = 1.26 \pm 0.05$; $\lambda_{\text{YSZ}+\text{WO}_3} = 1.65 \pm 0.15$ (W/m K)). L'addition de tungstène a une influence similaire sur la microdureté H . $H_{\text{YSZ}+\text{WO}_3}$ est de 12 à 15% plus élevée que H_{YSZ} . Les propriétés thermiques dans les couches de surface et au coeur de l'échantillon sont différentes. Cette même variation est également observée dans le cas de la microdureté H . Le dopage décroît rapidement le H dans les couches de surface, jusqu'à des valeurs inférieures à celles du coeur. Il en résulte que l'on peut estimer que le dopage de YSZ par WO_3 modifie de façon identique la structure de surface des grains céramiques et celle des monocristaux.

1 Introduction

In the last few years, much attention has been devoted to materials with the cubic fluorite structure and high ionic conductivity. They are interesting

from the point of view of basic research as well as for applications—for instance as potential materials for energy storage, fuel cells and for oxygen sensors.

Their application in industrial oxygen sensors is wide.¹ The determination of oxygen content in the melt, for instance, during the production of steel, enables the course of deoxidation and the final content of oxygen in the metals to be influenced from the technological point of view. In order to be economically effective, the oxygen sensor must have a high thermal shock resistance, in order to support the quench into the molten metal. Materials with a high ionic conductivity as well as a high thermal shock resistance are required. The addition of suitable impurities is a way to improve both the ionic conductivity and the thermal properties of stabilized ZrO_2 .

The aim of the present work is to investigate the influence of tungsten impurities on the thermal properties in connection with the microhardness of yttria-stabilized ZrO_2 .

2 Experiment

2.1 Preparation of samples

ZrO_2 and Y_2O_3 powders without and with an impurity of 1 wt% WO_3 were prepared by the Emitron Co. in Moscow. The specific surface of grains $\bar{\Pi}$ for the powder mixtures ZrO_2 – Y_2O_3 – WO_3 with regard to the WO_3 concentration were found to be: $\bar{\Pi}_{\text{YSZ}} = 2.55 \pm 0.07 \text{ m}^2/\text{g}$; $\bar{\Pi}_{\text{YSZ}+1 \text{ WO}_3 \text{ wt}\%} = 1.62 \pm 0.03 \text{ m}^2/\text{g}$ (Brunauer–Emmett–Teller method, Flow Sorb II 2300; Micromeritics Instrument Co., USA). The mixtures were homogenized in a dry corundum ball mill located in a rubber bag for 24 h, dry pressed at 100 MPa into the form of pellets in approximately 10 mm diameter cylinders of various heights (1 to 10 mm). The samples were sintered at 1680°C in air for 1 h. Single crystals were prepared by direct inductive melting in the cooling container.²

2.2 Microstructure of samples

The microstructure of ceramic samples was observed under TEM (Hitachi, HU-11A) at the accelerated voltage 75 kV using carbon replicas. The sintered samples were ground and polished using 15–0.25 μm diamond paste before observation under the electron microscope.

2.3 Elemental distribution in samples

The elemental distribution of Zr, Y, W and the impurity background of YSZ was examined on a microprobe (Jeol, JXA-5A). The preparation of samples was the same as for the investigation under the electron microscope.

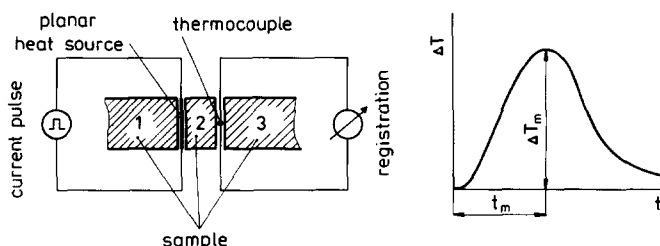


Fig. 1. Principle of the pulse method for the measurement of the thermal diffusivity and the specific heat. ΔT , Maximum of the temperature response to the heat pulse; t_m , time of the maximum of temperature response.

2.4 Density measurements

The pycnometric density ρ was investigated on a multi-volume pycnometer 1305 (Micromeritics Instruments Co., USA). The density was calculated from the mass of the sample and its volume. The volume of each pellet was determined on the principle of the He pressure change after gas pumping from a calibration cell to an expanding cell. Both of them have a known volume. The porosity of samples, measured on a porosimeter (Micromeritics pore sizer 9310), was found to be below the sensitivity limit of the equipment ($< 3\%$).

2.5 Thermal parameters

The pulse method of measurement of the thermal parameters is a dynamical method. The principle of this method is shown in Fig. 1. The planar heat source produces a thermal pulse in the sample. From the maximum of the temperature response and from the other parameters (input energy of the pulse, thickness of sample, etc.) the thermal diffusivity a and the specific heat c_p can be calculated. The formulae, from which these quantities are calculated, have been obtained by solving the heat-conduction differential equation.³ The thermal conductivity can be estimated as

$$\lambda = a \cdot \rho \cdot c_p \quad (1)$$

The basic characteristics of both measured types of ceramics are summarized in Table 1. The measured samples consist of three numbered pieces (X, Y, Z) with a specific arrangement, noted $X \parallel Y \mid Z$, in the holder (Fig. 1). The double line (\parallel) refers to the heat source and the single one (\mid) to the thermocouple ($1 \parallel 2 \mid 3$ in Fig. 1).

2.6 Measurement of microhardness

The microhardness was measured by the indentation method. The indentation was carried out at room temperature by means of diamond Vickers pyramide on a microscope (Neophot-21, Carl Zeiss, Germany). The loads on the indenter varied from 0.05 to 1 N. It allowed the determination of the microhardness of crystals at various distances from

Table 1. Characteristics of samples of ZrO_2 ceramics

Composition (mol%)	Density (kg/m^3)	Diameter (mm)	Height (mm)
8 Y_2O_3	5813	10.5	1–10
8 Y_2O_3 + 1 wt% WO_3	5764	11.5	4–10

the surface ($0.08\text{--}1.5\text{ }\mu\text{m}$). The faces $\{100\}$, $\{110\}$, $\{111\}$ were used for indentation. An average value of microhardness was estimated from the dimension of about 10 indenter impressions.

3 Results and Discussion

3.1 Structure of samples

The dependence of the lattice parameter of YSZ on the type of solid solution and on the WO_3 concentration was analysed by X-ray diffraction. The results obtained showed that both interstitial and substitutional sites are occupied by tungsten ions in the structure at the higher dopant concentrations. The proposal structure model of the solid solution was found to be in a good agreement with the measured physical properties.⁴

The quantitative microstructure analysis of ceramic samples was performed on TEM micrographs (Fig. 2) using a semi-automatic evaluation of microstructural parameters by means of a computer.⁵

The average grain size was larger for YSZ without tungsten: $8.31\text{ }\mu\text{m}$. The smaller grain size, $3.89\text{ }\mu\text{m}$, was observed for the sample containing the highest WO_3 concentration, 1 wt%.⁶ The grain size generally depends on the nature and on the concentration

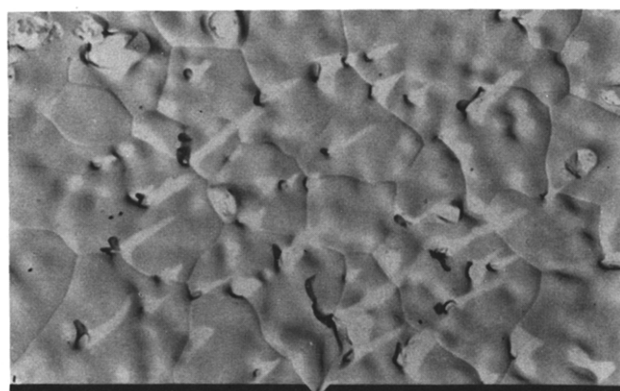


Fig. 2. Microstructure of YSZ + 1 wt% WO_3 sample sintered at 1680°C (TEM, magnification $\times 3000$).

of the impurity. It is well known that the solubility of transient element oxides in ZrO_2 is generally low. As can be seen in Ref. 7, it is also the case for WO_3 in YSZ. The excess tungsten oxide is accumulated at the grain boundary and in such way hinders the grain growth.

The elemental distribution of Zr, Y and W in all investigated samples is uniform. This can be seen in Fig. 3, which was chosen as the example. This result is in agreement with X-ray diffraction analysis. The formation of substitutional and interstitial solid solutions or their mutual coexistence, with tungsten addition, is performed in the basic cubic fluorite matrix without any influence on the elemental distribution. The impurity background of YSZ is negligible, with exception of Si from the starting powder. However, the amount of Si is, in comparison with the amount of W ($\geq 0.5\text{ wt}\%$), so small ($\leq 0.05\text{ wt}\%$) that no important influence of Si on the properties of YSZ is observable.

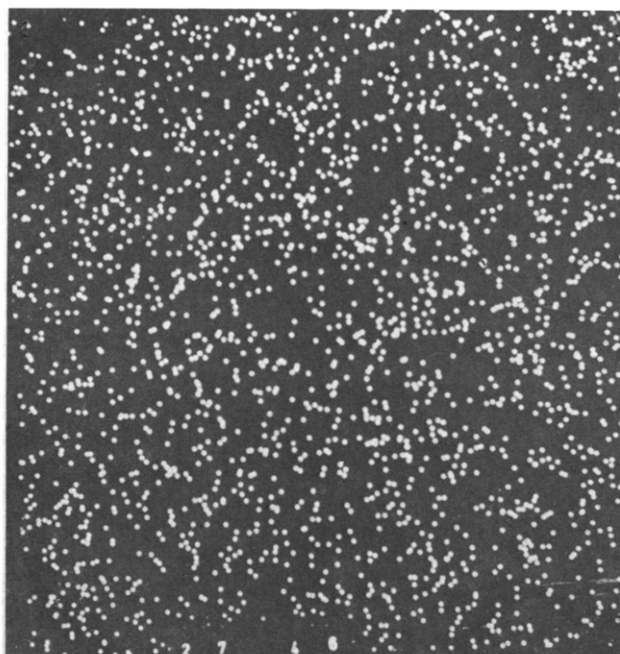


Fig. 3. Tungsten distribution in the YSZ + 1 wt% WO_3 sample (microprobe photos, magnification $\times 1200$).

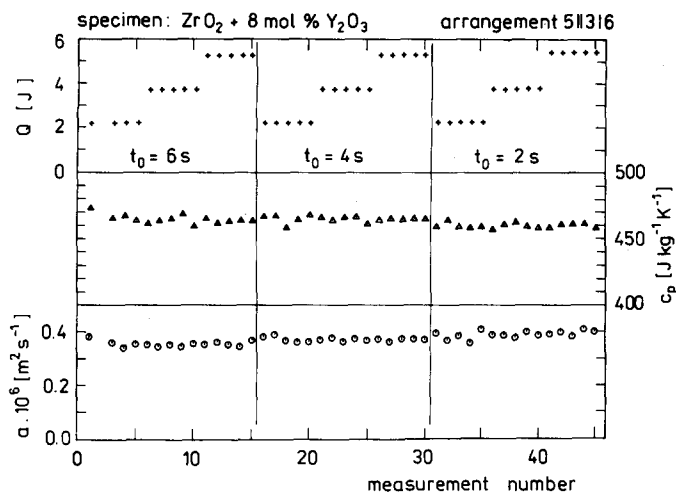


Fig. 4. A typical measured data set for determining the thermal properties of $\text{ZrO}_2 + 8 \text{ mol\% } \text{Y}_2\text{O}_3$ at room temperature. + + +, Input power of the heat pulse (top left); $\Delta\Delta\Delta$, specific heat (centre right); $\odot\odot\odot$, thermal diffusivity (bottom left).

3.2 Thermal diffusivity and specific heat

The thermal properties have been measured at 300 K under a vacuum of 10^{-3} Pa. More details about the sample holder and the analysis of the measurement errors are presented in Refs 8 and 9. A typical measured data set is given in Fig. 4. The program of a fully automatized apparatus changes the parameters of the heat pulse. Its input energy has been varied in the range of 2–6 J and the thermal pulse width in the range of 2–6 s (the upper part of Fig. 4). From such data sets the mean values and the root-mean square variations (rms) of c_p and a as a function of the sample arrangement have been calculated. The calculated mean values of c_p and a and corresponding root-mean square variations are plotted, for various sample arrangements, in Figs 5 to 8. The final values of c_p and a for YSZ and YSZ + WO_3 samples are also plotted on these figures. To compare the results with those of other authors, the data of zirconia ceramics with similar contents of ingredients are also shown^{10,11} (Table 2).

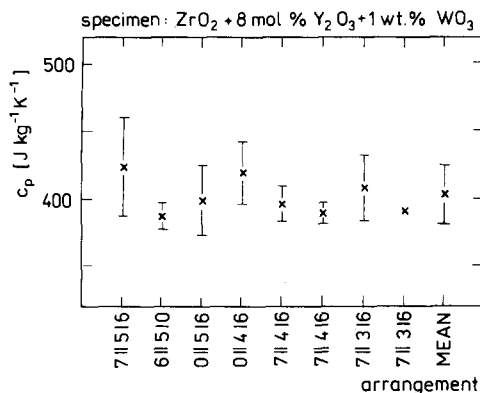


Fig. 5. Specific heat of $\text{ZrO}_2 + 8 \text{ mol\% } \text{Y}_2\text{O}_3 + 1 \text{ wt\% } \text{WO}_3$ for various arrangements of the samples. The last point on the right side of the figure represents the mean value of all the measurements.

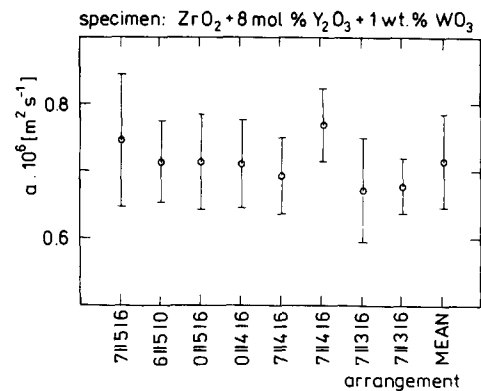


Fig. 6. Thermal diffusivity of $\text{ZrO}_2 + 8 \text{ mol\% } \text{Y}_2\text{O}_3 + 1 \text{ wt\% } \text{WO}_3$ for various arrangements of the samples. The last point on the right side of the figure represents the mean value of all the measurements.

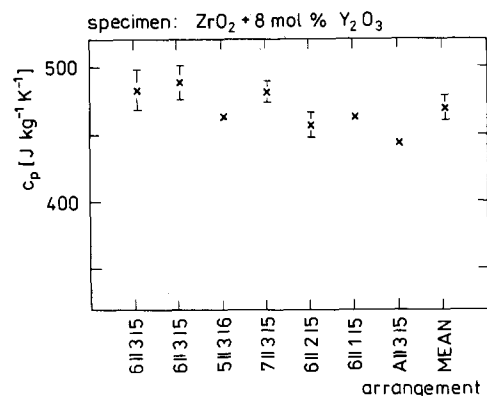


Fig. 7. Specific heat of $\text{ZrO}_2 + 8 \text{ mol\% } \text{Y}_2\text{O}_3$ for various arrangements of the samples. The last point on the right side of the figure represents the mean value of all the measurements.

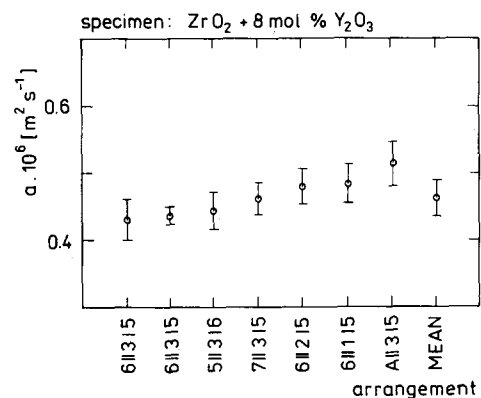


Fig. 8. Thermal diffusivity of $\text{ZrO}_2 + 8 \text{ mol\% } \text{Y}_2\text{O}_3$ for various arrangements of the samples. The last point on the right side of the figure represents the mean value of all the measurements.

Table 2. Thermal properties of Y_2O_3 -stabilized ZrO_2

Composition (mol%)	a $10^6 \text{ (m}^2/\text{s)}$	c_p (J/kg K)	λ (W/m K)
8 Y_2O_3	0.462 ± 0.026	470 ± 9	1.26 ± 0.05
8 Y_2O_3 + 1 wt% WO_3	0.714 ± 0.068	403 ± 22	1.65 ± 0.15
10 Y_2O_3	$0.7-0.89$	471	1.77 ± 2.36
12 Y_2O_3	0.6	—	—

From comparison of the thermal diffusivity of both sample types it can be seen that the specimen containing WO_3 has a higher value of a . The thermal diffusivity is a transport parameter which, in general, consists of the electron and phonon contributions. All of the ceramic samples are insulators at room temperature. Then the thermal diffusivity is $a = 1/3v_f l_f$, where v_f is an acoustic velocity and l_f is a free path of phonons. As the phonon-phonon interactions are predominantly at room temperature, the thermal diffusivity changes are influenced by acoustic velocity of phonons.⁸ This conclusion has been experimentally confirmed by the measurement of the microhardness, which is connected with the bulk modulus.¹² Since the determination of hardness of ceramic is not so easy, due to the presence of small grains ($\bar{D}_{\text{YSZ}+\text{WO}_3} = 3.89 \mu\text{m}$)—where \bar{D} is the average grain size—the microhardness values of 'pure' and doped single crystals of YSZ and of YSZ + WO_3 , respectively, have been measured and compared. It was shown that 1 wt% WO_3 increases the hardness by about 12–15%.

The structural analysis has confirmed that the ceramics are polycrystals.⁴ The volume ratio of atoms which are placed on the boundaries among the grains to the total volume of atoms in the sample is strongly dependent on the preparation technique. The grain boundaries are in a non-equilibrium state. A great contribution of anharmonic part of the specific heat exists for the structures which are in the non-equilibrium state.¹³ The contribution of this part of the grain to c_p is higher than that of the bulk of the grain which is closer to the thermodynamic equilibrium. The dependence of the c_p value on the sample thickness is plotted in Fig. 9. The samples with a thickness greater than 3 mm have a much higher value of c_p than those in which the thickness was reduced by grinding. This fact is caused by the inhomogeneities in the structure. It means that the surface layers have different thermal properties than the bulk of the sample. This conclusion has been confirmed by grinding part of the sample. The

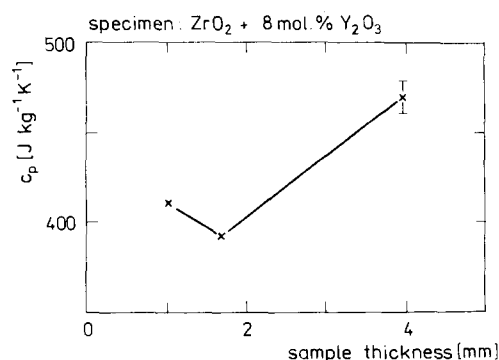


Fig. 9. Heat capacity of $\text{ZrO}_2 + 8 \text{ mol.\% Y}_2\text{O}_3$ as a function of the sample thickness.

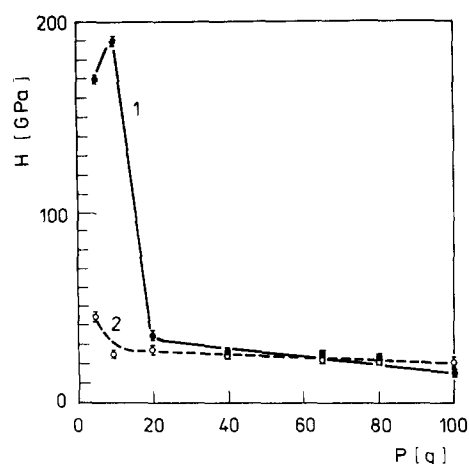


Fig. 10. Microhardness H as a function of load P applied to the indenter. 1, YSZ single crystal; 2, YSZ doped with 1 wt% WO_3 ($P = 5, 20$ and 100 g corresponds to the depth of penetration of the indenter into the crystal, i.e. $0.08, 0.5$ and $1.5 \mu\text{m}$, respectively).

ceramics containing 1 wt% WO_3 do not exhibit such types of structural inhomogeneities.

The similar difference in properties of the surface layers and the bulk of the sample was observed with the investigation of the hardness of these systems.

3.3 Microhardness (H)

The decrease of the microhardness H or increasing the load P on the indenter for the undoped (1) and doped (2) samples (1 wt% WO_3) can be seen in Fig. 10. The microhardness of the surface layer with the thickness $0.5 \mu\text{m}$ (at $P = 5\text{--}10 \text{ g}$) is more than one order of magnitude higher in comparison with the value of microhardness for the bulk of sample ($P \sim 100 \text{ g}$, $d_{\text{pen}} \sim 1.3\text{--}1.5 \mu\text{m}$ —where d_{pen} is the penetration depth of indenter). This difference in H is not dependent on the orientation of the sample surface, because the anisotropy of hardness of $\text{ZrO}_2\text{--Y}_2\text{O}_3$ crystals was found to be negligible. The addition of 1 wt% WO_3 sharply reduces the microhardness of the surface layer (2). It is possible that the addition of the tungsten impurity essentially changes the structure of surface layer ($0.5 \mu\text{m}$). It was also shown that the addition of 1 wt% WO_3 increases the microhardness H of the bulk by about 12–15%.

4 Conclusions

Comparing the thermal diffusivity a of both sample types, it can be seen that the sample containing WO_3 has a higher value of a ($a_{\text{YSZ}} = 0.462$; $a_{\text{YSZ}+\text{WO}_3} = 0.714 \times 10^6 \text{ m}^2/\text{s}$). It is assumed that this fact is caused by a higher phonon velocity.

The differences in properties of the surface layers and the bulk of single crystals were found by the investigation of the microhardness H and the

thermal diffusivity a . It was found that H of the surface layer ($0.5\ \mu\text{m}$) of undoped YSZ is different from H of the bulk of the sample by more than one order of magnitude. Doping sharply decreases H of the surface layers practically to the level of the bulk value ($\sim 15\ \text{GPa}$).

The difference in the specific heat (c_p) for both samples is higher than would follow from the difference in the composition. The results have shown that the addition of WO_3 decreases the average grain size from $\bar{D}_{\text{YSZ}} = 8.31\ \mu\text{m}$ to $\bar{D}_{\text{YSZ}+\text{WO}_3} = 3.89\ \mu\text{m}$. This allows the assumption that the change in c_p is connected with the change in the grain boundary surfaces, i.e. with the surface of the non-equilibrium phase.

The results allow the assumption that the doping of YSZ samples with WO_3 essentially changes the structure of the surface layers of grains in ceramics in a similar way to the surface layers in single crystals.

Acknowledgement

The authors are thankful to Dr Kubičár for many useful discussions and to Dr Morháčová for the determination of average grain size.

References

1. Nagata, K. & Goto, K. S., *Solid State Ionics*, **9–10** (1983) 1249.
2. Aleksandrov, V. I., Osiko, V. V., Prochorov, A. M. & Tatarintsev, V. M., *Uspechi Khimii*, **47** (1978) 385.
3. Krempaský, J., *Measurement of Thermophysical Properties*. Veda, Bratislava, 1969 (in Slovak).
4. Hanic, F., Hartmanová, M., Urusovskaya, A. A., Knab, G. G., Iofis, N. A. & Zyryanova, I. L., *Solid State Ionics*, **36** (1989) 197.
5. Morháčová, E., *Cryst. Res. Technol.*, **22** (1987) K159.
6. Morháčová, E., Hartmanová, M., Krcho, S., Hanic, F. & Travěnc, I., In *Proc. Int. Conf. on Engineering Ceramics '89*, Smolenice, 1989, p. 65.
7. Hartmanová, M., Travěnc, I., Putyera, K., Tunega, D., Urusovskaya, A. A., Korobkov, I. I. & Oreshnikova, T. V., *Mater. Sci. Forum*, **76** (1991) 19.
8. Kubičár, L., Pulse method of measuring basic thermophysical parameters. In *Wilson and Wilson's Comprehensive Analytical Chemistry*, Vol. 12, Part E, ed. G. Svehla. Elsevier-Veda, 1990, p. 341.
9. Kubičár, L. & Spišiak, J., *High Temp. High Press.*, **20** (1988) 619.
10. Youngblood, G. E., Rice, R. W. & Ingel, R. P., *J. Amer. Ceram. Soc.*, **71** (1988) 255.
11. Hasselman, D. P. H., Jonson, L. F., Bensen, L. D., Syed, R., Lee, H. L. & Swain, M. V., *Amer. Ceram. Soc. Bull.*, **66** (1987) 799.
12. Urusovskaya, A. A., In *Sovremennaja Kristallografija*. T.4, Nauka, Moskva, 1981, p. 47.
13. Spišiak, J., Kubičár, L. & Krivánková, D., *Int. J. Thermophys.*, **12** (1991) 593.